Journal of Applied Electrochemistry **34**: 823–831, 2004.

The influence of Ni content on the stability of copper–nickel alloys in alkaline sulphate solutions

KHALED M. ISMAIL[1]*, AHLAM M. FATHI[2] and WAHEED A. BADAWY[1]
[1]*Department of Chemistry, Faculty of Science, Cairo University, Giza-Egypt*
[2]*Department of Physical Chemistry, National Research Centre, Giza-Egypt*
*(*author for correspondence, e-mail: khaled966@hotmail.com)*

Received 28 June 2003; accepted in revised form 11 March 2004

Key words: alkaline, Cu–Ni, EIS, polarization, sulphate ions

Abstract

The electrochemical behaviour of copper–nickel alloys with different Ni content (5–65%) in sulphate solutions of pH 12 was investigated. The effects of temperature, immersion time, and concentration of sulphate ions were also studied. Different electrochemical methods such as open-circuit potential measurements, polarization techniques and electrochemical impedance spectroscopy (EIS) were used. Potentiodynamic measurements reveal that the increase in nickel content increases the corrosion rate of the alloy in sulphate solution linearly. Nevertheless, an increase in the nickel content along with increase in immersion time improves the stability of the Cu–Ni alloys due to the formation of a stable passive film. An equivalent circuit model for the electrode/electrolyte interface under different conditions was proposed. The experimental impedance data were fitted to theoretical data according to the proposed model. The relevance of the model to the corrosion/passivation phenomena occurring at the electrode/solution interface was discussed.

1. Introduction

Many of the alloys of copper are more resistant to corrosion than is copper itself, owing to the incorporation of corrosion resistant metals such as nickel [1]. Because of their extensive use in various environments many studies have been devoted to investigate the electrochemical behaviour of Cu–Ni alloys in neutral or slightly alkaline solutions [2–6]. Nevertheless, little work is reported concerning the effect of copper to nickel ratio [6, 7].

The electrochemical formation of passive layers on Cu–20Ni, Cu–50Ni and Ni–20Cu has been investigated in alkaline solution (1.0 M NaOH). A multilayer structure with an outer hydroxide, $Ni(OH)_2$, and an inner oxide layer underneath, consisting mainly of CuO was proposed [8], The film formed under open circuit conditions and at pH = 10 on a Monel 400 alloy was predominantly $Ni(OH)_2$ while at higher pH (14) the passive film was found to consist mainly of NiO [9].

Copper–nickels have been widely used in sea water environment because of their corrosion resistance [9, 10]. In many applications alkalis are added in boiler feed-water of power plants to inhibit pipe corrosion [1]. While many studies have been conducted in Na_2SO_4 and NaCl solutions, little work has been reported on the behaviour in Na_2SO_4 [11]. The present work is an investigation of the electrochemical behaviour of a variety of cupronickels in alkaline sulphate solutions intended to clarify the mechanism of the corrosion and passivation processes taking place at the electrode-electrolyte interface. The electrochemical behaviour of Cu–Ni alloys with 5, 10, 30 and 65% Ni (mass percent) was studied. Different electrochemical techniques, e.g., open-circuit potential measurements, polarization techniques and electrochemical impedance spectroscopy (EIS) were used.

2. Experimental details

The working electrodes were made from Cu–Ni rods and sheets, mounted into glass tubes by two-component epoxy resin leaving a surface area of 0.2 cm^2 to contact the solution. The materials used were commercial-grade Cu–Ni alloys of different Ni contents (5, 10, 30 and 65 mass% Ni). The cell was a conventional three-electrode all-glass electrochemical cell, with a platinum counter electrode and a saturated calomel reference electrode. Before each experiment, the working electrode was polished mechanically using successive grades of emery paper up to 1000 grit. The electrode was then rubbed with a smooth polishing cloth washed with triple distilled water and transferred quickly to the electrochemical cell. Electrochemical measurements were carried out in alkaline sulphate solution (0.25 M Na_2SO_4 + 0.01 M NaOH, pH 12).

The electrochemical impedance investigations and polarization measurements were performed using the Zahner Elektrik IM6 system. The potentials were referred to the saturated calomel electrode (SCE). All cyclic voltammetry measurements were carried out using a scan rate of 10 mV s^{-1}. For the calculation of the corrosion current density, i_{corr} and corrosion potential, E_{corr}, the potentiodynamic measurements were conducted at a scan rate of 1 mV s^{-1}. Details of the experimental procedures are described elsewhere [12, 13].

3. Results and discussion

3.1. *Open circuit potential measurements*

Open-circuit potentials of copper–nickel alloys with different Ni contents (5, 10, 30 and 65% Ni) were followed over 180 min in 0.25 M sulphate solutions of pH 12. For comparison, open-circuit potentials of the separate alloy constituents (copper and nickel) were also traced.

The steady state potential for copper (~ -50 mV) was attained within 100 min from electrode immersion in the sulphate solution while for nickel and alloys containing different Ni contents it took more than 150 min to reach steady state (cf. Figure la). Generally, the copper–nickel alloys show a continuous shift of the open-circuit potential towards less negative values, indicating additional passivation over the period of measurement (3 h). For all specimens, irrespective of the nickel content in the alloy, the measured steady state potential of the alloys varies from −140 to −170 mV. The steady state potential of Ni itself is about −150 mV.

The open-circuit potential of the Cu–65Ni alloy was followed over a period of 3 h in naturally aerated alkaline sulphate solutions of different concentrations. Typical results in a concentration range 0.05–1.0 M sulphate at pH 12 are presented in Figure. 1b. The steady state is reached within almost the same period of time (about 150 min) regardless of the sulphate concentration. Nevertheless, the steady state potential gets more negative with increasing the sulphate concentration, up to 0.15 M, before it starts to become less negative. This indicates that the passivation process depends on the sulphate ion concentration and it decreases to a minimum in the range 15–0.25 M Na_2SO_4 and then increases again with increase in the sulphate ion concentration.

3.2. *Potentiodynamic measurements*

Cyclic voltammograms for Cu, Ni, and Cu–Ni alloys with different Ni content were recorded at a scan rate of 10 mV s^{-1} in 0.25 M Na_2SO_4 solution of pH 12. A typical cyclic voltammogram for Ni in naturally aerated sulphate solution at 25 °C is shown in Figure 2a. The potential scan was initiated at −0.8 V, where a cathodic

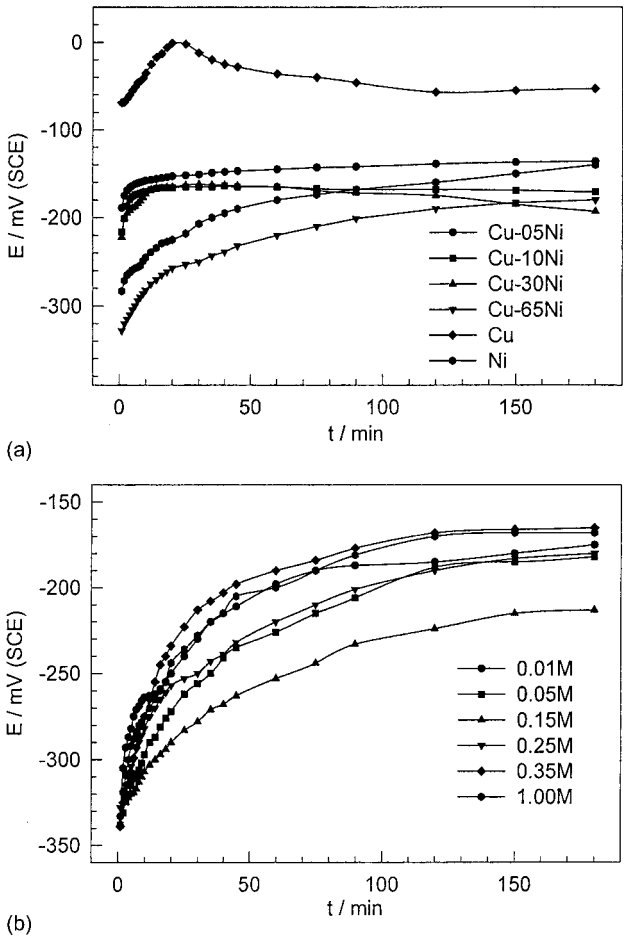

Fig. 1. (a) Variation of the open-circuit potential of Cu–Ni alloys with time in naturally aerated 0.25 M Na_2SO_4 solution, pH 12, at 25 °C. (b) Variation of the open-circuit potential of Cu–65Ni with time in Na_2SO_4 solution of different concentration, pH 12, at 25 °C.

current is observed due to hydrogen evolution (HER). After starting the positive-going sweep, the cathodic current density rapidly diminishes as the potential is made less negative. There is then the active region for metal dissolution, in which the current density increases slightly with potential.

On the anodic sweep, oxidation commenced at about −0.55 V followed by active anodic dissolution up to −0.42 V. It was reported that the predominant soluble nickel species in alkaline solutions are either $Ni(OH)^{+}_{(aq)}$ or $Ni^{2+}_{(aq)}$ ions [11, 14]. The dissolution of nickel has been reported to be pH-dependent, which suggests a contribution of OH^- to the active dissolution process [14, 15]. Considering the dependence of the active current density on OH^- concentration and the high OH^- concentration in alkaline solutions the overall anodic dissolution reactions can be represented as

$$Ni + OH^- \rightleftharpoons Ni(OH)_{ads} + e^- \quad (1a)$$

$$Ni + (OH)_{ads} \rightleftharpoons Ni(OH)^{+}_{aq} + e^- \quad (1b)$$

$$Ni + SO_4^{--} \rightleftharpoons NiSO_4 + 2e^- \quad (1c)$$

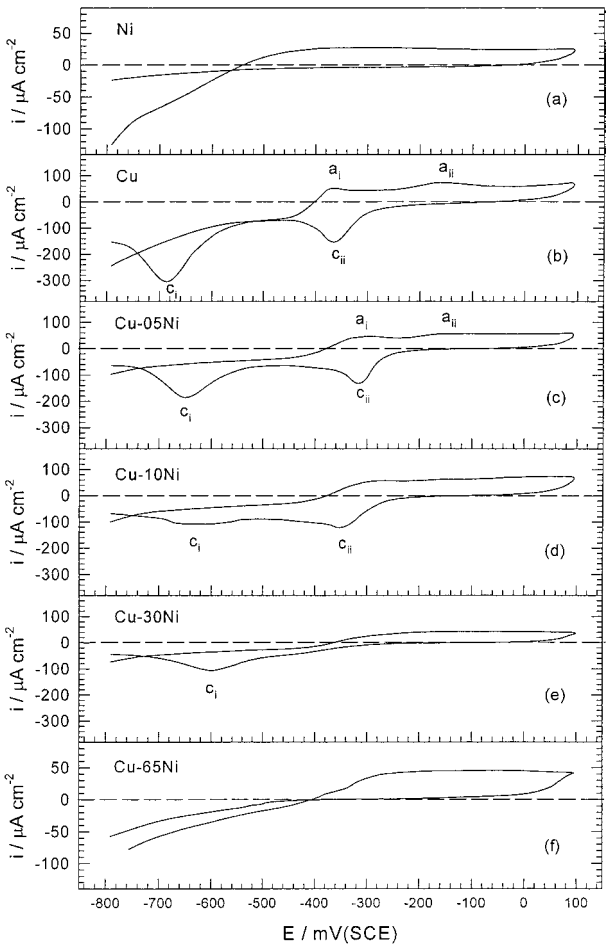

Fig. 2. Cyclic voltammograms of (a) Ni, (b) Cu, (c) Cu–5Ni, (d) Cu–10Ni, (e) Cu–30Ni, and (f) Cu–65Ni in 0.25 M Na_2SO_4 solution, pH 12, at 25 °C at a scan rate of 10 mV s^{-1}.

The film observed on Ni in a Na_2SO_4 solution, using optical and ESCA techniques, has been identified to be primarily $Ni(OH)_2$. At different values of pH and potential, NiO has been found to simultaneously with $Ni(OH)_2$ [9, 16]. The same primary step (1a) is assumed to be responsible for passivation

$$Ni(OH)_{ads} + OH^- \rightleftharpoons Ni(OH)_2 + e^- \quad (2a)$$

$$Ni(OH)_2 \rightleftharpoons NiO + H_2O \quad (2b)$$

Therefore, a layer of $Ni(OH)_2$ or NiO is formed directly from the metal dissolution. This layer is able to cause the recorded passivation region, in which the current density becomes stable with increasing potential. The difference between active dissolution according to (1b) and passivation according to (2a), is that in the former case the formation of $Ni(OH)_{adS}$ and their rapid transformation into Ni^{2+} is the process that determines the reaction rate, whereas in the passivation process the reaction with one hydroxyl ion is rapidly followed by reaction with the second [14].

Once the passive NiO film (or $Ni(OH)_2$) is formed, the anodic dissolution becomes steady at about 30 μA cm^{-2}. The dissolution process might be attributed either to electrochemical dissolution or to chemical dissolution of the oxide. Electrochemical dissolution is considered in the case of a reductive or oxidative dissolution of the oxide. Chemical dissolution depends on the solution pH, type of anions and temperature. For NiO the the dissolution is mostly a chemical process [17]. The specific influence of the anions on the passivation process can be explained in the following way. Specifically adsorbable anions displace the chemisorbed oxygen according to [14]

$$NiO + SO_4^{--} + H_2O \rightleftharpoons NiSO_4 + 2OH^- \quad (3)$$

The reverse potential scan does not show a cathodic peak corresponding to the reduction of the passive film. This can be attributed to either the high stability of the passive film or the overlap of the reduction of dissolved oxygen and passive film just preceding the potential range of the hydrogen evolution reaction [18].

A cyclic voltammogram for Cu in naturally aerated 0.25 M Na_2SO_4 solution, pH 12, at 25 °C is shown in Figure 2b. The potential scan was initiated at −0.8 V, where a considerable cathodic current is observed due to hydrogen evolution. There is then a transition region before the active region for metal dissolution, which is most probably due to the formation of adsorbed species such as $Cu(SO_4)^{--}_{ads}$ and/or $Cu(OH)^-_{ads}$ at the electrode surface [19, 20] via the reactions:

$$Cu + SO_4^{--} \rightleftharpoons Cu(SO_4)^{--}_{ads} \quad (4a)$$

$$Cu + OH^- \rightleftharpoons Cu(OH)^-_{ads} \quad (4b)$$

Usually, when several types of anion are present in the electrolyte, they compete for adsorption sites at the metal surface. Their varying adsorption at the surface might change the surface characteristics significantly. Enhanced adsorption of anions on anodized metal may promote dissolution or passivation with increasing potential [21]. The metal acquires a passive behaviour due to the formation of the adsorbed layer of the intermediate species [20]. This type of passivity is termed as pseudo-passivation.

The $Cu(SO_4)^{--}_{ads}$ and/or $Cu(OH)^-_{ads}$ species represent an adsorbed intermediate for active dissolution. In the anodic active region copper goes into solution as Cu^+ ions [22], the current density is continuously increasing with potential. The increase in anodic current can be attributed to dissolution of the adsorbed layer which can be described as follows:

$$Cu(OH)^-_{ads} + OH^- \rightleftharpoons Cu(OH)^-_{2(aq.)} + e^- \quad (5a)$$

$$2Cu(SO_4)^{--}_{ads} \rightleftharpoons Cu_2(SO_4)_{(aq.)} + SO_4^{--} + 2e^- \quad (5b)$$

It is a reasonable assumption to hold the same primary steps (4b and 5a) as being responsible for passivation,

i.e., the formation of a passive film of Cu_2O. An anodic peak is recorded at ~ -0.35 V (a_i)

$$2Cu(OH)^-_{2(aq.)} \rightleftharpoons Cu_2O + H_2O + 2OH^- \quad (6a)$$

$$2Cu(OH)^-_{ads} \rightleftharpoons Cu_2O + H_2O + 2e^- \quad (6b)$$

The second anodic peak (a_{ii}) at ~ -0.16 V can be attributed to the conversion of the outer layer of the oxide film, Cu_2O, at the oxide-solution interface to the Cu(II) oxide or a hydrated oxide [23], according to

$$Cu_2O + H_2O \rightleftharpoons 2CuO + 2H^+ + 2e^- \quad (7a)$$

$$Cu_2O + 3H_2O \rightleftharpoons 2Cu(OH)_2 + 2H^+ + 2e^- \quad (7b)$$

The potential scan in the negative direction shows two cathodic peaks at -0.36 V (c_{ii}) and -0.68 V (c_i). The cathodic peak (c_{ii}) is attributed to the electro-reduction of $Cu(OH)_2$ while peak (c_i) is related to the electro-reduction of Cu_2O [23].

Cyclic voltammograms for Cu–5Ni, Cu–10Ni, Cu–30Ni and Cu–65Ni alloys in alkaline 0.25 M Na_2SO_4 solution are presented in Figure 2c–f. Their shape resembles more the voltammograms recorded for the metal representing the main alloy component. However, in the case of alloys the values of the dissolution anodic current density and consequently the cathodic current density decrease with increasing Ni content. The electrochemical behaviour of the alloys has the characteristic properties of both alloy components. On the anodic sweep for Cu–5Ni and Cu–10Ni (cf. Figure 2c and d), oxidation commences at about -0.38 V showing a significant anodic current with two small anodic peaks. This means that the passive film formed has low protection properties. The cyclic voltammogram exhibits anodic peak (a_i) at ~ -0.3 V and another anodic peak (a_{ii}) at -0.16 V, which can be attributed to the formation of Cu(I) and Cu(II) compounds, respectively. The reverse potential scan shows two cathodic peaks at -0.35 V (c_{ii}) and -0.65 V (c_i) corresponding to the reduction Cu(II) to Cu(I) and Cu(I) to Cu, respectively [24].

For Cu–30Ni and Cu–65Ni (cf. Figure 2e and f), oxidation commences at about -0.38 V. The cycic voltammograms did not show the two anodic peaks (a_i) and (a_{ii}). While no cathodic peaks were observed for Cu–65Ni during the cathodic scan, an ill-defined cathodic peak at about -0.38 V and another clear one at -0.6 V were recorded for Cu–30 Ni. It seems that the presence of nickel reduces the dissolution of copper due to the formation of a compact passive film of NiO at the electrode surface.

3.3. *The corrosion rates of Cu–Ni alloys*

The behaviour of the Cu–Ni alloy with various nickel contents was investigated in 0.25 M alkaline sulphate solution. Using potentiodynamic polarization data the values of the corrosion current density, i_{corr} and corrosion potential, E_{corr} were calculated, and the potentiodynamic polarization curves are presented in Figure 3a.

It should be noted that the corrosion current density, i_{corr}, measured at the moment of electrode immersion in the solution, increases with increasing Ni content (cf. Figure 3b), and that the increase in Ni content does not produce any significant change in the corrosion potential. On the other hand, the measured corrosion current after 3 h of electrode immersion decreases with increase in Ni content. This result can be explained on the basis of the dissolution of Ni with the formation of Ni^{2+} followed by the formation of a barrier layer of $Ni(OH)_2$ or NiO according to Equations 2b and 2c. After reaching the steady state, the ability of the barrier film to impart passivity depends on the amount of NiO in the barrier layer which, in turn, depends on the Ni content. The corrosion behaviour of the alloy after long immersion time is controlled by the passivating properties of

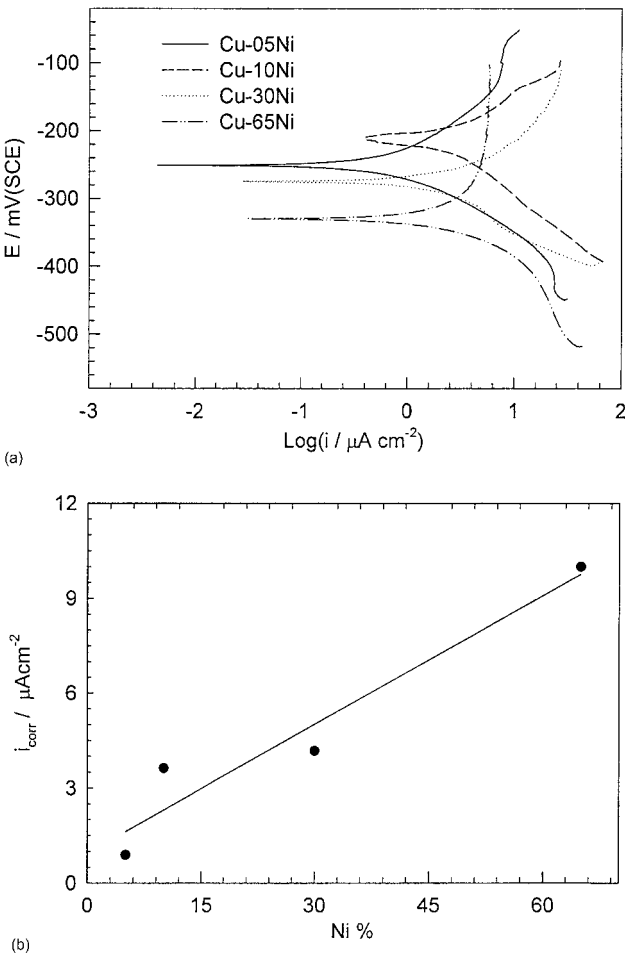

Fig. 3. (a) Potentiodynamic polarization curves of Cu–Ni alloys in 0.25 M Na_2SO_4 solution, pH 12, at 25 °C at a scan rate of 10 mV s^{-1} (b) Corrosion current density after immediate immersion of Cu–65Ni alloy in 0.25 M Na_2SO_4 solution, pH 12, at 25° C as a function of the Ni content.

Ni and hence the corrosion current density decreases as the Ni-content increases.

The corrosion rate of various Cu–Ni alloys in alkaline sulphate solutions of different concentrations was recorded. For all studied Cu–Ni alloys, the corrosion current density, i_{corr}, increases with increasing sulphate ion concentration up to about 0.15–0.25 M (cf. Figure 4). For sulphate ion concentration higher than 0.25 M the corrosion rate decreases, most probably due to the formation of passive layers.

3.4. *Effect of temperature on the corrosion rates of Cu–Ni alloys*

The effect of temperature on the corrosion rates of copper, nickel, Cu–5Ni and Cu–65Ni was investigated in naturally aerated 0.25 M Na_2SO_4 solution of pH 12. From the potentiodynamic Tafel polarization data obtained at quasi-stationary conditions at different temperatures, the value of the corrosion current density, i_{corr}, was calculated. A small influence of temperature on the corrosion behaviour of nickel and cupronickel alloys was recorded while a remarkable effect was observed in the case of copper. A temperature rise of about 30 °C slightly increases (1.2–1.5 times) the rate of corrosion of nickel and cupronickel alloys, whereas in the case of copper the rate of corrosion increases five fold. In general, the corrosion rate, which is represented by the corrosion current density, i_{corr}, increases with increasing temperature, and the process obeys the familiar Arrhenius equation [25].

$$\frac{\mathrm{d}\log i_{corr}}{\mathrm{d}T} = \frac{E_a}{RT^2} \tag{8}$$

where E_a is the molar activation energy and R the gas constant (8.314 J mol^{-1} K^{-1}). The Arrhenius plots are presented in Figure 5, and the values of activation energy, E_a, were calculated according to Equation 8. The calculated E_a values are 34.8, 10.2, 4.1, and 10.1 kJ mol^{-1} for Cu, Ni, Cu–5Ni and Cu–65Ni, respectively. Such low activation energy value (less than 40 kJ mol^{-1}) is an indication that the dissolution (corrosion) process is under diffusion control [26].

3.5. *The electrochemical impedance measurements of Cu–Ni alloys*

To get further information concerning the influence of the alloying element on the corrosion process, the effect of nickel content in the alloy was investigated using electrochemical impedance spectroscopy. The impedance data recorded after 180 min immersion in 0.25 M Na_2SO_4 solutions of pH 12 are presented in Figure 6a. The Bode plots of four alloys with different Ni content (5, 10, 30, and 65%) show a narrow phase maximum at intermediate frequencies for alloys with low Ni content (5 and 10) indicating the formation of less protective film and a broad phase maximum with increasing Ni content (30 and 65) reflecting the formation of a more protective film [12]. Moreover, the impedance values of the different alloys in sulphate solutions were found to depend on the Ni content (cf. Figure 6a). An increase in Ni content improves the stability of the alloy in sulphate. Presumably a sufficient density of Ni atoms is required at the alloy surface to form a continuous passive film which improves the corrosion resistance of the alloy.

The impedance data were analyzed using software provided with the impedance system where the dispersion formula was used (9). For a simple equivalent circuit model consisting of a parallel combination of a capacitor, C_{dl}, and a resistor, R_{ct}, in series with a resistor, R_s, representing the solution resistance, the electrode impedance Z is represented by

$$Z = R_s + \frac{R_{ct}}{1 + (2\pi f R_{ct} C_{dl})^{\alpha}} \tag{9}$$

where α denotes an empirical parameter ($0 \leq \alpha \leq 1$) and f is the frequency in Hz. The above relation is known as

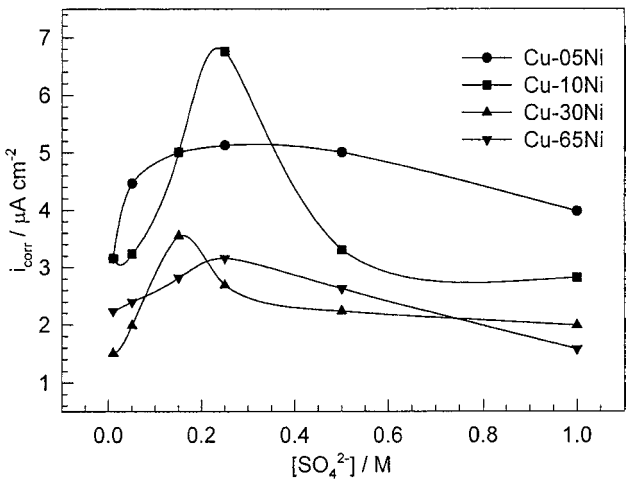

Fig. 4. Corrosion current density of Cu–Ni alloys in Na_2SO_4 solution of different concentrations, pH 12, at 25 °C.

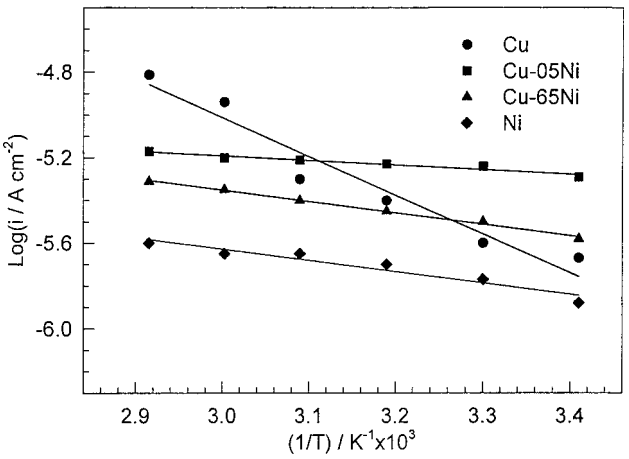

Fig. 5. Arrhenius plots of the corrosion of Cu, Ni, Cu–5Ni and Cu–65Ni alloys in 0.25 M Na_2SO_4 solution, pH 12.

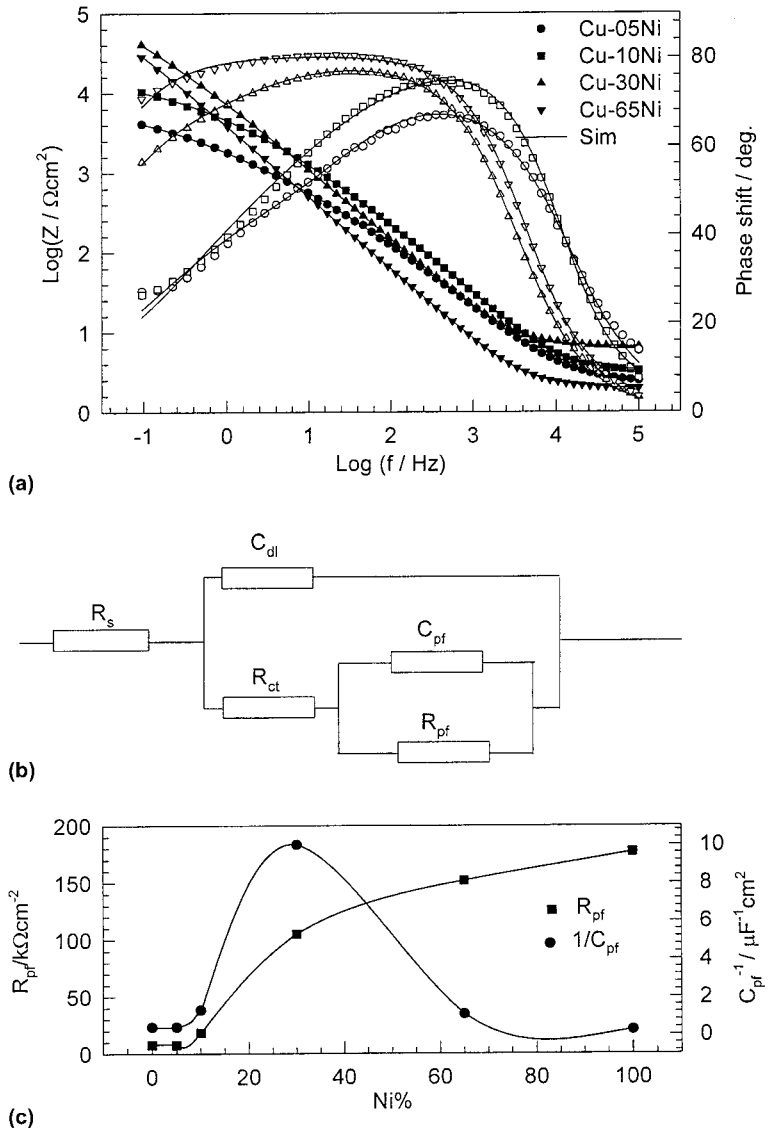

Fig. 6. (a) Bode plots of Cu–Ni alloys after 180 min of electrode immersion in 0.25 M Na_2SO_4 solution, pH 12, at 25 °C. (b) Equivalent circuit used in the fitting of the impedance data of Cu–Ni alloys, R_s = solution resistance, R_{ct} = charge transfer resistance, C_{dl} = double layer capacitance, R_{pf} = passive layer resistance, and C_{pf} = passive layer capacitance. (c) The resistance and relative thickness of the passive layer on Cu–Ni alloys in 0.25 M Na_2SO_4 solution, pH 12, as a function of Ni content.

the dispersion formula and takes into account the deviation from the ideal RC-behaviour in terms of a distribution of time constants due to surface inhomogeneties, roughness effects, and variations in properties or compositions of surface layers [18, 27, 28]. The impedance data of alloys with different nickel content were analyzed using the equivalent circuit shown in Figure 6b where another $R_{pf}C_{pf}$ combination was introduced to account for the presence of surface film. The calculated equivalent circuit parameters for alloys with different Ni content are presented in Table 1. The change of the passive layer capacitance, C_{pf}, can be used as an indicator of a change in this layer thickness, d. The reciprocal capacitance of the passive layer, $1/C_{pf}$, is directly proportional to its thickness [13]. The resistance, R_{pf}, and the thickness, $1/C_{pf}$, of the passive layer increase with increase in Ni content. For higher Ni-content e.g. Cu–65Ni the decrease in the thickness with increased passivity can be attributed to the formation of a compact film which consists mainly of NiO. It is noteworthy that the value of α for Cu, Cu–5Ni and Cu–10Ni is in the region of 0.5 (cf. Table 1). This indicates the presence of a diffusion process at the interfacial. Such diffusion process may indicate a reversible dissolution process which is accompanied by the formation of a porous film. It seems that passive film formation under open-circuit conditions proceeds through a dissolution-precipitation mechanism [12, 20]. The time constant at high frequencies originates from the $R_{ct}C_{dl}$ combination while that at low frequencies initiates from the $R_{pf}C_{pf}$ combination. The passive layer resistance, R_{pf}, increases with increase in Ni content (cf. Figure 6c). This means that increase in Ni content improves the corrosion resistance.

Table 1. Equivalent circuit parameters for Cu–Ni alloys with different Ni content after 180 min of electrode immersion in 0.25 M Na_2SO_4 solution of pH 12 at 25 °C

Ni%	R_s /Ω	C_{dl} /μF cm^{-2}	α_1	R_{ct} /Ω cm^2	C_{pf} /μF cm^{-2}	α_2	R_{pf} /kΩ cm^2
0	10.7	4.7	0.80	1027	2.50	0.50	7.7
5	11.9	6.2	0.89	5.76	2.49	0.50	7.5
10	5.1	4.5	0.89	5.61	0.77	0.50	18.3
30	12.7	7.9	0.85	5.57	0.10	0.80	105.2
65	10.0	19.2	0.89	2.04	0.92	0.99	151.8
100	10.8	12.4	0.93	1.56	3.98	0.88	177.1

The experimental results obtained with the Cu–65Ni alloys at different electrode immersion times are presented as Bode plots in Figure 7a. The initial impedance (Z) recorded 2 min after electrode immersion drifts continuously towards increasing values. The increase in the impedance values is due to progressive passive film formation until a steady state is achieved. Although the value of $1/C_{pf}$ shows a continuous decrease, the value of R_{pf} for the Cu–65Ni alloy shows a continuous increase with increasing immersion time (cf. Figure 7b and Table 2). This indicates a change in the passive film structure and/or composition. In such cases, the most probable explanation is dissolution of the relatively thick outer (porous) layer of the passive film and growth of the thin (compact) and more passive film.

The experimental Bode plots obtained with the Cu–65Ni electrode after 180 min of electrode immersion in solutions with different concentrations of sulphate ions (0.05–1.0 M and pH 12) are presented in Figure 8a. The recorded impedance data show a decrease in the impedance values with increasing sulphate concentration up to 0.25 M before they start to increase with further increase in the sulphate concentration. Using the equivalent circuit shown in Figure 6b, the calculated

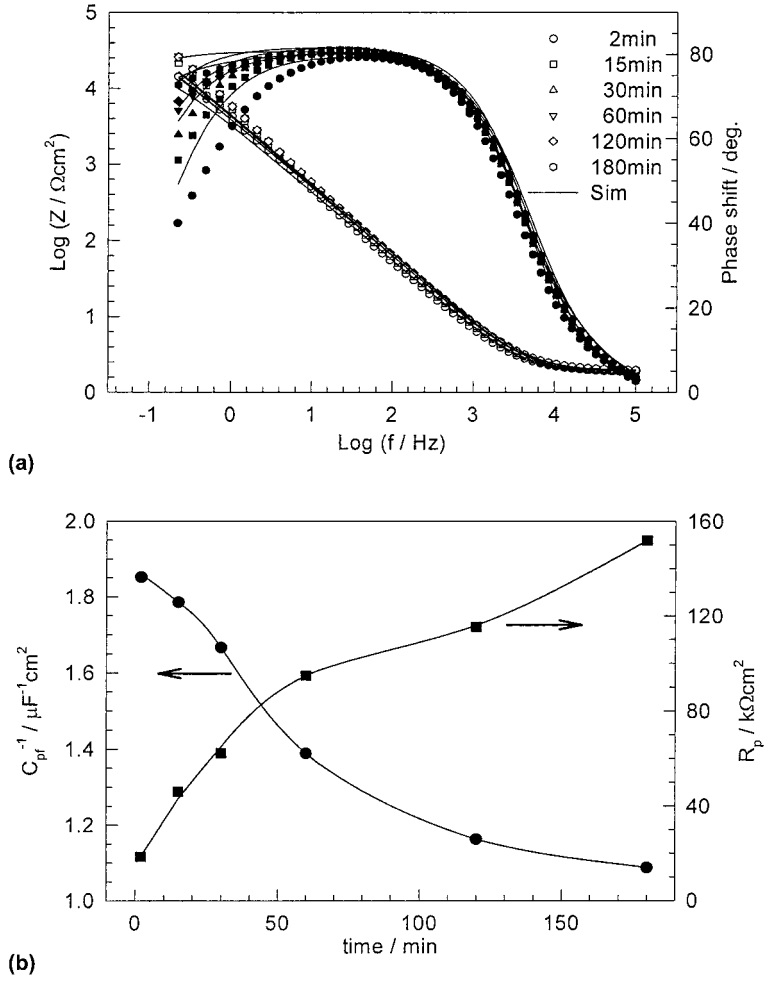

Fig. 7. (a) Bode plots of Cu–65Ni alloy after different immersion times in 0.25 M Na_2SO_4 solution, pH 12, at 25 °C. (b) The resistance and relative thickness of the passive layer on Cu–Ni alloys in 0.25 M Na_2SO_4, solution pH 12.

Table 2. Equivalent circuit parameters for Cu–65Ni electrode in 0.25 M Na_2SO_4 solution of pH 12 at different time intervals at 25 °C

Time /min	R_s /Ω	C_{dl} /μF cm^{-2}	α_1	R_{ct} /Ω cm^2	C_{pf} /μF cm^{-2}	α_2	R_{pf} /kΩ cm^2
2	9.5	25.4	0.89	5.4	0.54	0.98	18.5
15	9.5	22.4	0.90	4.9	0.56	0.97	46.1
30	9.7	22.0	0.90	3.4	0.60	0.98	62.3
60	9.8	22.0	0.91	3.0	0.72	0.98	94.9
120	9.7	19.9	0.89	2.0	0.86	0.98	115.4
180	10.0	19.2	0.89	2.0	0.92	0.99	151.8

parameters for Cu–65Ni after 180 min of electrode immersion in solutions with different concentrations of sulphate ions (pH 12) are presented in Table 3.

Figure 8b shows non monotonic variations of the passive layer resistance, $R_{pf,}$ and the relative passive layer thickness, $1/C_{pf}$, with sulphate ion concentration. A minimum value of the passive layer resistance, R_{pf}, and a maximum value of the relative passive layer thickness, $1/C_{pf}$, were recorded at about 0.25 M. In sulphate ion concentrations higher than 0.25 M the passive layer resistance increases again while the passive layer thickness decreases with concentration. This indicates that the passive film formed in low sulphate concentrations is thick and non-resistive whereas the film formed in high sulphate concentrations is thin and resistive. It is clear that the results obtained from the analysis of the electrochemical impedance measurements is consistent with the open-circuit and potentiodynamic measurements which show the highest corrosion rate of the alloys in sulphate solutions with intermediate concentration (0.15–0.25 M).

4. Conclusions

- The electrochemical behaviour of the copper–nickel alloys in alkaline sulphate solutions resembles that of the main component of the alloy and the corrosion resistance increases with increasing nickel content.

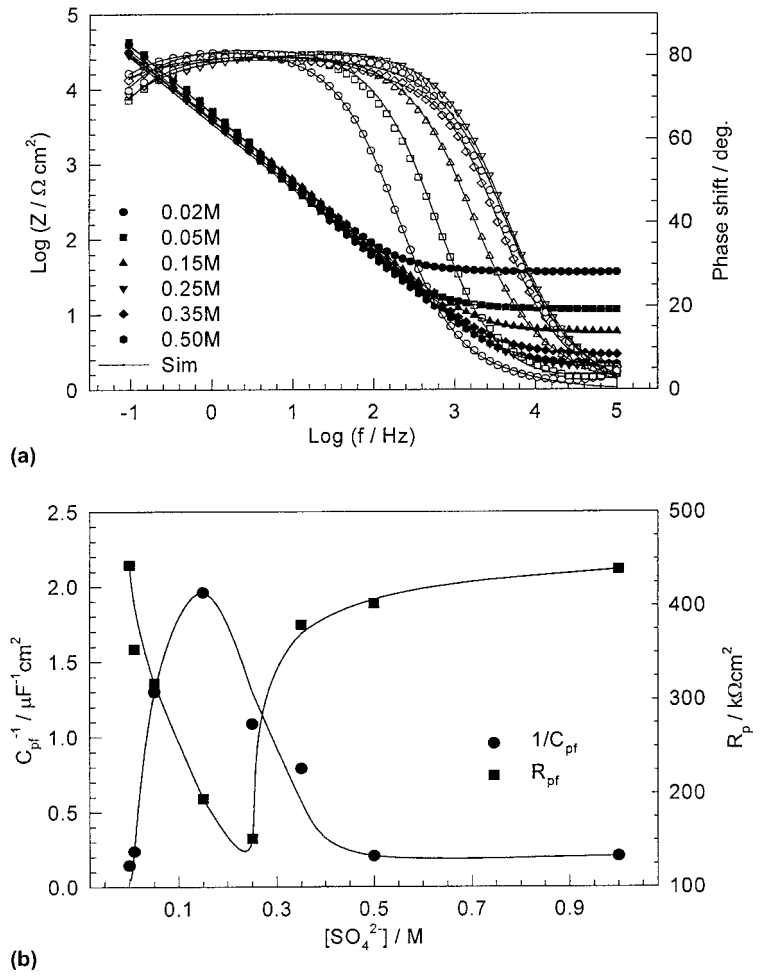

Fig. 8. (a) Bode plots of Cu–65Ni alloy after 180 min of immersion in Na_2SO_4 solution of different concentration, pH 12, at 25°C. (b) The resistance and relative thickness of the passive film on Cu–Ni alloys in Na_2SO_4 solution of different concentration, pH 12.

Table 3. Equivalent circuit parameters for Cu–65Ni alloy after 180 min of electrode immersion in Na_2SO_4 solution of different concentration of pH 12 at 25 °C

$[SO_4^-]$ /M	R_s /Ω	C_{dl} /μF cm^{-2}	α_1	R_{ct} /Ω cm^2	C_{pf} /μF cm^{-2}	α_2	R_{pf} /kΩ cm^2
0.01	97.2	17.3	0.90	41.9	4.22	0.80	353.6
0.05	68.0	17.8	0.95	7.3	0.77	0.98	317.2
0.15	30.3	14.5	0.89	5.2	0.51	0.99	194.6
0.25	10.0	19.2	0.89	2.1	0.92	0.99	151.8
0.35	15.2	18.4	0.89	3.0	1.26	0.96	302.4
0.50	11.8	12.1	0.89	3.0	4.86	0.90	402.4
1.00	6.4	14.4	0.89	1.7	4.87	0.90	438.8

- Long immersion of the different copper–nickel alloys in the solution increases the passive film resistance.
- There is a critical concentration of alkaline sulphate at which the corrosion resistance is very low.

Acknowledgements

The AvH foundation (Bonn-Germany) and University of Cairo (Egypt) are gratefully acknowledged for providing the impedance system.

References

1. L.L. Shreir, R.A. Jarman and G.T. Burstein (Eds), 'Corrosion: Metal/Environment Reaction', 3rd edn (Butterworth-Heinemann Ltd, Linacre House, Jorden Hill, Oxford OX2 8DP, reprinted 1995), p. 4:41, 17:70 and 17:84.
2. P.K. Chauhan and H.S. Gadiyar, *Corros. Sci.* **25** (1985) 55.
3. A.M. Beccaria and J. Crousier, *Br. Corr. J* **24** (1989) 49.
4. H.P. Hack and H.W. Pickering, *J. Electrochim. Soc.* **138** (1991) 690.
5. M. Metikos-Hukovic and *I.* Milosev, *J. Appl. Electrochem.* **22** (1992) 448.
6. I. Milosev and M. Metikos-Hukovic, *Electrochim. Acta* **42** (1997) 1537.
7. A.N. Kamkin, A.D. Davydov, G.-D. Zhou and V.A. Marichev, *Russ. J. Electrochem.* **35** (1999) 531.
8. P. Druska, H.-H. Strehblow and S. Golledge, *Corros. Sci.* **38** (1996) 835.
9. N.S. Mclntyre, T.E. Rummery, M.G. Cook and D. Owen, *J. Electrochim. Soc.* **123** (1976) 1164.
10. D.D. Macdonald, B.C. Syrett and S.S. Wing, *Corrosion* **34** (1978) 289.
11. J.A. Ali and J.R. Ambrose, *Corros. Sci.* **32** (1991) 799.
12. K.M. Ismail and W.A. Badawy, *J. Appl. Electrochem.* **30** (2000) 1303.
13. K.M. Ismail, A.A. El-Moneim and W.A. Badawy, *J. Electrochem. Soc.* **148** (2001) C81.
14. U. Ebersbach, K. Schwabe and K. Ritter, *Electrochim. Acta* **12** (1967) 927.
15. N. Sato and G. Okamoto, *in* J.O'M. Bockris, B.E. Conway, E. Yeager and R.E. White (Eds), 'Comprehensive Treatise of Electrochemistry', Vol. 4, (Plenum Press, New York, 1981), p. 201.
16. R.E. Hummel, R.J. Smith and E.D. Verink Jr. *Corros. Sci.* **27** (1987) 803.
17. G. Dagan and M. Tomkiewicz, *J. Electrochem. Soc.* **139** (1992) 461.
18. A.E. Bohe, J.R. Vilche, K. Juettner, W.J. Lorenz and W. Paatsch, *Electrochim. Acta* **34** (1989) 1443.
19. L.M. Rice-Jackson, G. Horanyi and A. Wiekowski, *Electrochim. Acta* **36** (1991) 753.
20. K.M. Ismail, S.S. El-Egamy and M. Abdelfatah, *J. Appl. Electrochem.* **31** (2001) 663.
21. V.P. Parkhutik, J.M. Albella and J.M. Martinez-Duart, *in* B.E. Conway, J.O'M. Bockris and R.E. White (Eds), 'Modern Aspects of Electrochemistry', Vol. 23, (Plenum Press, New York, 1992), p. 330.
22. A. Jardy, A. Legal Lasalle-Molin, M. Keddam and H. Takenouti, *Electrochim. Acta* **37** (1992) 2195.
23. H.-H. Strehblow and B. Titze, *Electrochim. Acta* **25** (1980) 839.
24. J. Morals, G.T. Fernandez, P. Esparza, S. Gonzalez, R.C. Salvarezza and A.J. Arvia, *Corros. Sci.* **37** (1995) 211.
25. P.W. Atkins, 'Physical Chemistry', 5th edn, (Oxford University Press, Oxford, 1994), p. 877
26. A. Wieckowski and E. Ghali, *Electrochim. Acta* **30** (1985) 1423.
27. K. Hladky, L.M. Calow and J.L. Dawson, *Br. Corr. J* **15** (1980) 20.
28. J. Hitzig, J. Titz, K. Juettner, W.J. Lorenz and E. Schmidt, *Electrochim. Acta* **29** (1984) 287.